Available online at www.sciencedirect.com
ScienceDirect
International Journal of Sediment Research 23 (2008) 315-328
INTERNATIONAL JOURNAL OF SEDIMENT RESEARCH
www.elsevier.com/locate/ijsrc

One-dimensional numerical simulation of non-uniform sediment transport under unsteady flows

Hongwei FANG[1], Minghong CHEN[2], and Qianhai CHEN[3]

Abstract

One-dimensional numerical models are popularly used in sediment transport research because they can be easily programmed and cost less time compared with two- and three-dimensional numerical models. In particular, they possess greater capacity to be applied in large river basins with many tributaries. This paper presents a one-dimensional numerical model capable of calculating total-load sediment transport. The cross-section-averaged sediment transport capacity and recovery coefficient are addressed in the suspended load model. This one-dimensional model, therefore, can be applied to fine suspended loads and to hyperconcentrated flows in the Yellow River. Moreover, a new discretization scheme for the equation of unsteady non-uniform suspended sediment transport is proposed. The model is calibrated using data measured from the Yantan Reservoir on the Hongshui River and the Sanmenxia Reservoir on the Yellow River. A comparison of the calculated water level and river bed deformation with field measurements shows that the improved numerical model is capable of predicting flow, sediment transport, bed changes, and bed-material sorting in various situations, with reasonable accuracy and reliability.

Key Words: One-dimensional numerical model, Sediment transport capacity, Recovery coefficient, Adaptation length, Unsteady flow

1 Introduction

One-dimensional numerical simulation is an important tool in recent sediment transport research. Many steady and stepwise quasi-steady one-dimensional models have been widely used. They have been tested in engineering practice in reservoirs and rivers, for the deposition and erosion. The HEC-6 model was introduced for sediment movement under quasi-steady flows in gravel-bed rivers (Thomas, 1982). Chang (1982) presented a model for erodible channels. Han (1980) provided a method for non-equilibrium transport of non-uniform suspended load. Van Niekerk et al. (1992) developed a model to simulate erosion and deposition in a relatively straight, non-bifurcating alluvial channel. In this model, the individual size-density fractions of bed material were considered. Many unsteady models have also been developed and applied for estuaries and other geographical features. Cunge et al. (1980) introduced unsteady model equations derived from the Saint-Venant hypotheses to simulate river flood wave propagation. Armanini and Di Silvio (1988), and Bell and Sutherland (1983), provided models for movable bed channels. Rahuel et al. (1989) developed and tested a new computational methodology for the fully coupled simulation of unsteady water and sediment movement in alluvial rivers. In their methodology, the non-uniform bed load transport was studied, and sorting and armoring effects was

[1] Prof., Dept. of Hydraulic Engineering, Tsinghua Univ., State Key Laboratory of Hydroscience and Engineering, Beijing, 100084, China
[2] PhD, College of Water Conservancy and Civil Engineering, China Agricultural Univ., Beijing 100083, China. Corresponding author, E-mail: chenminghong@cau.edu.cn
[3] Engineer, Institute of the Yangtze River Research, Wuhan, 430010, China
Note: The original manuscript of this paper was received in May 2007. The revised version was received in April 2008. Discussion open until Dec. 2009.

considered. Wu et al. (2004) and Wu (2004) further refined this model to simulate the non-equilibrium transport of non-uniform total load under unsteady flow conditions in dendritic channel networks with hydraulic structures.

The problems addressed in this paper involve non-uniform sediment transport under unsteady flows. One test case is the Hongshui River in China, in which 90% of sediment transported is suspended load. The particle size of the suspended load ranges from 1mm to 0.001mm, with a median diameter of 0.015mm. The size range of the bed load is from 400mm to 0.1mm. Another test case is the Yellow River. Most of the annual sediment load in the Yellow River is transported in a few flood events caused by heavy rains. This pattern sometimes results in hyperconcentrated flows with sediment concentrations up to several hundred kilograms per cubic meter and even in excess of one thousand kilograms per cubic meter. In the middle reach of the Yellow River and its tributaries, the difference in the annual sediment load could be as high as eightfold, and sediment load transported in the peak five-day period may constitute as much as 30–50% of the total annual load. In general, the smaller the watershed area, the more pronounced is the aforementioned phenomenon (Zhang and Xie, 1993).

Owing to the problems outlined above, research on non-uniform sediment transport still requires considerable development. At present, non-uniform sediment transport is usually evaluated by sorting particles into several uniform particle groups, which may give relatively accurate results for low sediment concentration transport but not for high sediment concentration transport. Furthermore, hyperconcentrated flow results in highly unsteady sediment transport. Thus, research on discretization schemes for unsteady sediment transport equations is a considerable challenge. In this paper, a new method is developed to characterize the behavior of non-uniform sediment transport under unsteady flows.

2 Mathematical model

2.1 Governing equations

The unsteady water flow dynamics in a channel can be described by the Saint-Venant equations:

$$\frac{\partial A}{\partial t}+\frac{\partial Q}{\partial x}=q \tag{1}$$

$$\frac{\partial Q}{\partial t}+\frac{\partial}{\partial x}\left(\frac{Q^2}{A}\right)+gA\frac{\partial Z}{\partial x}+g\frac{Q|Q|}{C^2AR}=0 \tag{2}$$

where x and t are spatial and temporal axes; Q is flow discharge; A is flow area; q is the side discharge per unit channel length; g is gravitational acceleration; C is the Chezy coefficient, defined as $C=\frac{1}{n}R^{1/6}$, with n being the Manning coefficient of roughness; R is the hydraulic radius; and Z is water surface elevation.

The sediment transport can be separated as suspended load and bed load according to sediment transport models, or as bed-material load and wash load according to sediment sources. Basically, the former separation is more widely adopted in actual cases.

The governing equation for the non-equilibrium transport of suspended load (Han, 1980) is

$$\frac{\partial (AS)}{\partial t}+\frac{\partial (QS)}{\partial x}+\alpha\omega B(S-S_*)=0 \tag{3}$$

where S is the cross-section-averaged sediment concentration; S_* is the cross-section-averaged sediment transport capacity; α is the recovery coefficient relating to adaptation from a non-equilibrium state to the equilibrium state; ω is the sediment settling velocity; and B is the channel width.

The governing equation for the non-equilibrium transport of bed load (Phillips and Sutherland, 1989) is

$$\frac{\partial G_b}{\partial x}+\frac{1}{L_s}\left(G_b-G_{b*}\right)=0 \tag{4}$$

where L_s is the adaptation length for bed load transport; and G_b and G_{b*} are the actual bed load transport rate and bed load transport capacity, respectively.

Combining suspended load and bed load leads to the total bed deformation equation:

$$\rho'\frac{\partial A_0}{\partial t}+\alpha\omega B(S-S_*)+\frac{1}{L_s}\left(G_b-G_{b*}\right)=0 \tag{5}$$

where ρ' is the dry density of sediment; and $\frac{\partial A_0}{\partial t}$ is the change rate of deposition area.

2.2 Recovery coefficient

For a low concentration flow, the recovery coefficient and section-averaged sediment transport capacity can be calculated using the methods of Han (1980), and Zhang and Xie (1993). Based on results obtained from validation tests in many reservoirs and rivers, it has been suggested that $\alpha = 1$ for the case of erosion and $\alpha = 0.25$ for deposition. However, some rivers have flows with particularly high concentrations of sediment, such as the Yellow River and its tributaries; the maximum recorded sediment concentration to date was 1,650kg/m^3 (Chien and Wan, 1988). The recovery coefficient should be upgraded and readjusted for such flow. In the model for hyperconcentrated flow, the physical meaning of the recovery coefficient under equilibrium transport conditions is

$$\alpha = \frac{\omega_b \left(s_b - s_{b*} \right)}{\omega \left(S - S_* \right)} \tag{6}$$

where the subscript *b* indicates variable values near the channel bed.

The sediment concentration and sediment transport capacity near the river bed are evaluated by the depth-averaged values and by the relative concentration profile. Supposing that the concentration profile can be applied to the distribution of the sediment transport capacity, one can integrate the concentration profile over the water depth (Zhang and Xie, 1993) and obtain

$$\frac{S}{s_b} = \frac{S_*}{s_{b*}} = \int_{\eta_a}^{\eta_h} \exp\left\{ \frac{\omega}{\kappa u_*} \left[f(\eta) - f(\eta_a) \right] \right\} d\eta \tag{7}$$

where $f(\eta)$ is the function of the sediment concentration profile; $\eta = 1 - \frac{y}{h}$; η_a and η_h are the relative positions of the river bed and surface, respectively.

For the lower boundary layer with high sediment concentration, ω_b can be adjusted as follows (Fei, 1991).

$$\frac{\omega_b}{\omega} = \left(1.0 - \beta' S_v \right)^{m'} \tag{8}$$

where S_v is the sediment concentration by volume; and $m' = 2.5$ and $\beta' = 1.77$ for uniform sediment.

Combining Eqs. (6), (7) and (8) leads to the recovery coefficient:

$$\alpha = \frac{\left(1.0 - \beta' S_{vi} \right)^{m'}}{\int_{\eta_a}^{\eta_h} \exp\left\{ \frac{\omega_i}{\kappa u_*} \left[f(\eta) - f(\eta_a) \right] \right\} d\eta} \tag{9}$$

2.3 Sediment transport capacity

Cao (1979) presented an improved sediment transport capacity formula for suspended load based on Zhang's (1961) formula:

$$S_* = K \left(\frac{\gamma_m}{\gamma_s - \gamma_m} \frac{U^3}{gR\omega} \right)^m \tag{10}$$

where γ_m is the density of the sediment-laden flow; γ_s is the density of sediment; *K* and *m* are empirical parameters; and ω is the settling velocity of sediment determined by $\omega = \left(\sum_{i=1}^{n} p_i \omega_i^m \right)^{1/m}$ for non-uniform sediment, with p_i being the size fraction.

The sediment transport capacity formulas proposed by Meyer-Peter and Mueller (1948), Yalin (1972), Engelund and Fredsoe (1976), are often used to calculate the discharge of uniform bed load. These formulas are also capable of predicting the total discharge of non-uniform bed load. Meyer-Peter and Mueller's formula proved to be more efficient in characterizing the bed load movement and it is expressed as

$$g_{b*}=\frac{\left[\left(\frac{k_s}{k_r}\right)^{3/2}\gamma hJ-0.047(\gamma_s-\gamma)D_m\right]^{3/2}}{0.125\left(\frac{\gamma}{g}\right)^{1/2}\left(\frac{\gamma_s-\gamma}{\gamma_s}\right)} \tag{11}$$

where D_m is the average grain size of the bed load; J is the energy slope; $k_s=\frac{U}{h^{3/2}J^{1/2}}$; and $k_r=\frac{26}{D_{90}^{1/6}}$.

2.4 Non-equilibrium adaptation length

The adaptation length for bed-load transport, L_s, originally introduced as an empirical parameter with a unit of length, has been significantly redefined by many researchers. It is often set as the saltation step length (Phillips and Sutherland, 1989). According to Einstein (1942), the average saltation step length of the bed load is determined using $L_s=l_s d_m/(1-P_e)$, in which l_s is the non-dimension step length, d_m is the particle size of the bed load, and P_e is the percentage of sediment on the channel bed. Yalin (1972) supposed the average saltation step length would be a function of the Shields number, defined as $L_s=\alpha\theta$, in which α is a constant and $\theta=\tau_c/(\gamma_s-\gamma)d_m$. In the mathematical model of Phillips and Sutherland (1989), the saltation step length is given as $L_s=100d_{50}$. van Rijn (1984) also established formulas that were applied in many numerical models. However, Rahuel et al. (1989) set L_s as once or twice the numerical grid length in the case of natural rivers. Wu et al. (2004) and Wu (2004) suggested that the bed-load adaptation length is related to the length of the dominant bed forms, which may be a function of flow depth or channel width. In the present study, $L_s=0.73B$ is used, which is similar to the relation used by Wu (2004) but with a different coefficient.

3 Numerical solution methods

3.1 Solution for flow equations

Eqs. (1) and (2) are discretized using the Preissmann implicit four-point finite difference method, and the discretized equations are solved using the pentadiagonal matrix algorithm. During the iteration process, one may assume $A_j^{n+1}=A_j^*+\Delta A_j$ and $Q_j^{n+1}=Q_j^*+\Delta Q_j$, in which the symbol * denotes variable values at the last iteration step, ΔA and ΔQ are the increments of flow area and discharge, respectively. Substituting these two relations into the discretized Eqs. (1) and (2) and linearizing the nonlinear terms leads to the following iteration relations.

$$a_{1j}\Delta Q_j+b_{1j}\Delta Z_j+c_{1j}\Delta Q_{j+1}+d_{1j}\Delta Z_{j+1}=e_{1j} \tag{12}$$

$$a_{2j}\Delta Q_j+b_{2j}\Delta Z_j+c_{2j}\Delta Q_{j+1}+d_{2j}\Delta Z_{j+1}=e_{2j} \tag{13}$$

where a_{1j} to e_{1j} and a_{2j} to e_{2j} are coefficients related to hydraulic parameters, geometry and time. Eqs. (12) and (13) are solved by successively applying the double sweep Thomas algorithm.

3.2 Solution for the suspended load transport equation

To approximate the suspended sediment transport equation (Eq. (3)), many schemes have been developed. One scheme is neglecting the time-dependent term of Eq. (3). Therefore, the quasi-steady transport of sediment is assumed. The computation time subsequently decreased. The commonly used equation for calculating sediment concentration of this scheme (Han, 1980) was

$$S=S_*+(S_0-S_{0*})e^{-\frac{\alpha\omega\Delta x}{Q_b}}+(S_{0*}-S_*)\frac{Q_b}{\alpha\omega\Delta x}\left(1-e^{-\frac{\alpha\omega\Delta x}{Q_b}}\right) \tag{14}$$

where Q_b is the unit discharge, defined as $Q_b=Q/B$; Δx is the reach length; and the subscript 0 denotes variables of the upstream section.

If the time-dependent term is considered, Eq. (3) can be reformulated as

$$\frac{\partial S}{\partial t}+\frac{Q}{A}\frac{\partial S}{\partial x}+\frac{\left(q+\alpha\omega B\right)S}{A}-\frac{\alpha\omega BS_*}{A}=0 \tag{15}$$

The characteristic method is used to solve Eq. (15):

$$S=\frac{A}{q+\alpha\omega B}e^{f\left(x-\frac{Q}{A}t\right)-\frac{q+\alpha\omega B}{A}t}+\frac{\alpha\omega B}{q+\alpha\omega B}S_* \tag{16}$$

where $f\left(x\right)$ is a function to be determined.

Considering the initial condition at $t = 0$, one can obtain the function f:

$$f\left(x\right)=\ln\left\{\frac{q+\alpha\omega B}{A}\left(\left[S-S_*\right]_x^0+\left[\frac{q}{q+\alpha\omega B}S_*\right]_x^0\right)\right\} \tag{17}$$

Consequently, substituting this function into Eq. (16) yields

$$\left[S\right]_x^t=\left[S_*\right]_x^t+\left[S-S_*\right]_{x-\frac{Q}{A}t}^0e^{-\frac{q+\alpha\omega B}{A}t}+\left[\frac{q}{q+\alpha\omega B}S_*\right]_{x-\frac{Q}{A}t}^0e^{-\frac{q+\alpha\omega B}{A}t}-\left[\frac{q}{q+\alpha\omega B}S_*\right]_x^t \tag{18}$$

The above expression (18) implies that the sediment concentration at the downstream node involves (1) the average sediment transport capacity of the downstream node; (2) the difference between the sediment concentration and averaged sediment transport capacity of the considered river reach; and (3) the side flow discharge.

Assuming that the average sediment transport capacity is constant locally at the reach and substituting the continuity equation for q, one can obtain

$$\left[S\right]_x^t=\left[S_*\right]_x^t+\left[S-S_*\right]_{x-\frac{Q}{A}t}^0e^{-\frac{q+\alpha\omega B}{A}t}-\left[\frac{1}{q+\alpha\omega B}\left(\frac{\partial Q}{\partial x}+\frac{\partial A}{\partial t}\right)S_*\right]_x^t\left(1-e^{-\frac{q+\alpha\omega B}{A}t}\right) \tag{19}$$

Using the discretized forms of $\frac{\partial Q}{\partial x}$ and $\frac{\partial A}{\partial t}$ yields

$$\begin{aligned}\left[S\right]_x^t=&\left[S_*\right]_x^t+\left[S-S_*\right]_{x-\frac{Q}{A}t}^0e^{-\frac{q+\alpha\omega B}{A}t}-\left[\frac{1}{q+\alpha\omega B}\left(\frac{Q}{\Delta x}+\frac{A}{\Delta t}\right)S_*\right]_x^t\left(1-e^{-\frac{q+\alpha\omega B}{A}t}\right)\\&+\left[\frac{1}{q+\alpha\omega B}\left(\frac{Q}{\Delta x}\right)S_*\right]_{x-\Delta x}^t\left(1-e^{-\frac{q+\alpha\omega B}{A}t}\right)+\left[\frac{1}{q+\alpha\omega B}\left(\frac{A}{\Delta t}\right)S_*\right]_x^{t-\Delta t}\left(1-e^{-\frac{q+\alpha\omega B}{A}t}\right)\end{aligned} \tag{20}$$

Eq. (20) is used for uniform sediment transport; i.e., the settling velocity ω is constant. It can be extended to non-uniform sediment transport. Therefore, the sediment concentrations for each size class can be computed individually using Eq. (20).

The fractional sediment concentration and capacity can be expressed as $S_i = p_iS$ and $S_{*i} = p_{*i}S_*$, respectively. Here, p_{*i} is the gradation of the sediment transport capacity, which is assumed to equal the gradation of the suspended load concentration (Han, 1980). Thus, the non-uniform sediment concentration can be obtained by summing Eq. (20) over all size classes:

$$\begin{aligned}\left[S\right]_x^t=&\left[S_*\right]_x^t+\left[S-S_*\right]_{x-\frac{Q}{A}t}^0\left[\sum_{i=1}^n p_ie^{-\frac{q+\alpha\omega_iB}{A}t}\right]_{x-\frac{Q}{A}t}^0+\left[\frac{AS_*}{\Delta t}\sum_{i=1}^n p_i\frac{1-e^{-\frac{q+\alpha\omega_iB}{A}t}}{q+\alpha\omega_iB}\right]_x^{t-\Delta t}\\&-\left[\left(\frac{Q}{\Delta x}+\frac{A}{\Delta t}\right)S_*\sum_{i=1}^n p_i\frac{1-e^{-\frac{q+\alpha\omega_iB}{A}t}}{q+\alpha\omega_iB}\right]_x^t+\left[\frac{QS_*}{\Delta x}\sum_{i=1}^n p_i\frac{1-e^{-\frac{q+\alpha\omega_iB}{A}t}}{q+\alpha\omega_iB}\right]_{x-\Delta x}^t\end{aligned} \tag{21}$$

Han (1980) proposed a scheme to calculate the gradations of suspended load and bed material. The cases of sedimentation and erosion were handled differently. In the case of erosion, denoting the percentage of eroded bed material at the surface layer as λ, one can derive the gradation of suspended load as

$$P_i = \frac{P_{0i} - \lambda p_i^*}{1-\lambda} \tag{22}$$

where P_{0i} is the initial gradation of bed material and p_i^* is the gradation of suspended load entrained from bed material, defined as

$$p_i^* = R_{0i} \frac{1-(1-\lambda^*)^{(\frac{\omega_{zh}}{\omega_i})^\beta}}{\lambda^*} \tag{23}$$

where λ^* is the thickness ratio of the mixing layer and eroded subsurface layer; R_{0i} is the gradation of bed material; β is a parameter often given as 0.75; and ω_{zh} is the effective settling velocity of the sediment mixture, satisfying the following relation.

$$\frac{\sum_{i=1}^{n} R_{0i}[1-(1-\lambda^*)^{(\frac{\omega_{zh}}{\omega_i})^\beta}]}{\lambda^*} = 1 \tag{24}$$

After bed erosion, the gradation of bed material becomes

$$R_i = R_{0i} \frac{(1-\lambda^*)^{(\frac{\omega_{zh}}{\omega_i})^\beta}}{1-\lambda^*} \tag{25}$$

where the effective settling velocity ω_{zh} can be obtained from

$$\frac{\sum_{i=1}^{n} R_{0i}(1-\lambda^*)^{(\frac{\omega_{zh}}{\omega_i})^\beta}}{1-\lambda^*} = 1 \tag{26}$$

For the situation of deposition, denoting the deposition ratio as λ, one derives the gradation of suspended load as

$$P_i = P_{0i} \frac{(1-\lambda)^{(\frac{\omega_i}{\omega_{zh}})^\beta}}{1-\lambda} \tag{27}$$

where ω_{zh} must satisfy

$$\frac{\sum_{i=1}^{n} P_{0i}(1-\lambda)^{(\frac{\omega_i}{\omega_{zh}})^\beta}}{1-\lambda} = 1 \tag{28}$$

After deposition, the gradation of bed material becomes

$$R_i = \frac{P_{0i}}{\lambda}[1-(1-\lambda)^{(\frac{\omega_i}{\omega_{zh}})^\beta}] \tag{29}$$

In the above expressions, the calculation of ω_{zh} is very complicated. It has to be calculated iteratively according to Eqs. (24), (26) and (28).

3.3 Solution for the bed load transport equation

Both the finite difference method and the characteristic method can be used to solve the bed-load transport equation, i.e., Eq. (4). However, because of the absence of the time-dependent term, the characteristic method appears to be simpler. The analytical solution of this equation is

$$G_b = G_{b*} + \left(G_{b0} - G_{b0*}\right)e^{-\frac{\Delta x}{L_s}} + \left(G_{b0*} - G_{b*}\right)\frac{L_s}{\Delta x}\left(1 - e^{-\frac{\Delta x}{L_s}}\right) \tag{30}$$

4 Study cases

The model developed above was applied to (i) the Yantan Reservoir on the Hongshui River, which has a sediment-laden flow; and (ii) the Sanmenxia Reservoir on the Yellow River, which has a hyperconcentrated sediment flow.

4.1 Yantan reservoir calculations

The Yantan Reservoir is located on the Hongshui River. This river is about 150 km long with a drainage basin of 8,080 km^2. The Panyang River is its largest tributary. Seventy cross sections are studied for the Yantan Reservoir, from the upstream Tian'e Station to the dam site, including 13 sections in the Panyang branch, as can be seen in Fig. 1.

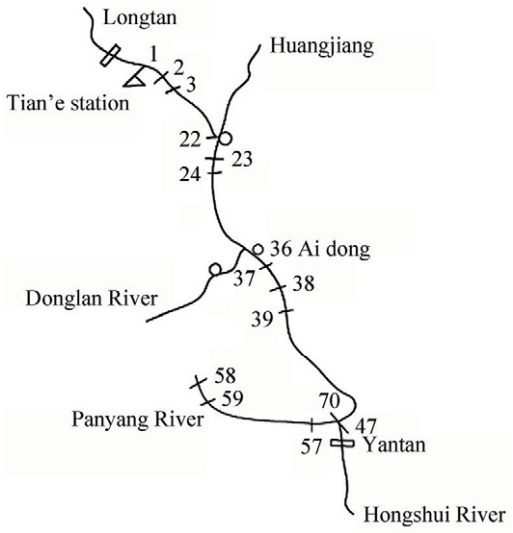

Fig. 1 Sketch of the Hongshui River

Boundary conditions

The measured flow discharge $Q(t)$ and sediment discharge $S(t)$ from 1994 to 2002 at Tian'e Station, the first hydrology station in this drainage basin, are used as the inlet boundary condition. Similar boundary conditions are used for the Panyang River. The downstream boundary condition is the time series of water elevations at the Yantan Dam site during the same period.

Topographic data from 1994 for all cross-sections, from the Tian'e Station to the Yantan Dam site, are used as the initial bed level. Other topographic data from 1997, 1999 and 2001 are also used to validate this model.

Supplemental relations for turbidity density current

High-concentration sediment-laden flow in the reservoir may form a density current that moves along the channel bottom. Having sufficient energy to overcome all resistances, the density current moves to the dam site and even exits the reservoir. The sediment transport capacity of the density current is much larger than that of clear water; hence this current could carry more sediment in much coarser size.

The density current plunging into the reservoir is related to the conditions of flow and sediment. Abundant data show that the physical condition in the section of the plunging point is (Zhang, 1961)

$$u^2 \Big/ \eta_g g H \le 0.6 \tag{31}$$

where u and H are the section-averaged flow velocity and depth, respectively; and η_g is a modification factor for gravity, defined as $\eta_g = \dfrac{r'-r}{r'}$, in which $r' = r + \left(1 - \dfrac{r}{r_s}\right) S$, with r', r and r_s being the bulk densities of muddy water, clear water and sediment, respectively.

When density current deposition occurs, the averaged velocity and sediment concentration should be adjusted. There are two types of density currents: positive slope density current and inverse slope density current. If the positive slope density current occurs (Zhang, 1961), the velocity and depth of the density current are

$$u' = \sqrt[3]{8\eta_g g Q_b J_0 / f'} \quad \text{and} \quad h' = \sqrt[3]{\frac{f'}{8\eta_g}\frac{Q_b^2}{gJ_0}} \tag{32}$$

where J_0 is the slope of the river bed, defined as $J_0 = \Delta Z_0 / \Delta X$, and f' is an empirical parameter given as 0.022.

If inverse slope density current occurs (Qin et al., 1995), the velocity and depth of the density current are

$$u' = \frac{1}{K_1}\sqrt{\eta_g (1-K_1)^3 H} - u \quad \text{and} \quad h' = K_1 H \tag{33}$$

where K_1 equals 0.55 empirically.

When the plunging point is determined, the time (T_1) for the density current to reach the dam site equals the distance from the plunging point to the dam site over the velocity of the density current. If the flood lasts for less than T_1, the density current does not arrive at the dam site. The velocity of density current is adjusted by using Eqs. (32) or (33). And the sediment transport capacity of density current is adjusted by using Eq. (10).

Supplemental relation for flocculation

In the calculations for the Yantan Reservoir, the particles with sizes smaller than 0.03mm are found to flocculate. For non-uniform fine clay, the following relationship between the flocculation factor F and particle size D can be established (Zhang and Liang, 1994).

$$F = K' D^{n'} \tag{34}$$

where $K' = 0.41$ and $n' = -0.28$. The size gradation of flocculation can then be determined. Table 1 shows the relationship between particle size and settling velocity determined by Eq. (34).

Table 1 Relation of particle size and settling velocity

Particle size (mm)	F	Flocculation size (mm)	Settling velocity (m/s)	Flocculation settling velocity (m/s)
0.5	1.0	0.5	67.2×10^{-3}	67.2×10^{-3}
0.075	1.0	0.075	5.06×10^{-3}	5.06×10^{-3}
0.0325	1.0	0.0325	0.95×10^{-3}	0.95×10^{-3}
0.0175	1.27	0.0222	0.28×10^{-3}	0.44×10^{-3}
0.0075	1.61	0.012	0.05×10^{-3}	0.13×10^{-3}
0.005	1.81	0.009	0.022×10^{-3}	0.073×10^{-3}
0.0025	2.19	0.005	0.006×10^{-3}	0.022×10^{-3}
0.001	2.84	0.003	0.0009×10^{-3}	0.008×10^{-3}

Water level results

The calculated water levels for 1994 and 1999 are compared with the observed data. The Yantan Dam was built in 1994, therefore, the results of 1994 characterize the original natural state. The results of 1999 show the situation when the river was closed and deposition occurred. A comparison of the calculated and measured water surfaces in 1994 and 1999 is shown in Fig. 2. It can be seen that, because the reservoir was in a natural condition before 1994, the water surface had a steep slope along the river. After the dam was constructed, the water level rose, and the slope of the water surface became gentle. In these two cases, the calculations agree well with the measurements.

Sedimentation results

To compare the calculated and measured depositions in the reservoir, a total of 57 cross sections along the main stream are grouped into four regions. Calculated and measured volumes of deposition after eight years of reservoir operation are listed in Table 2.

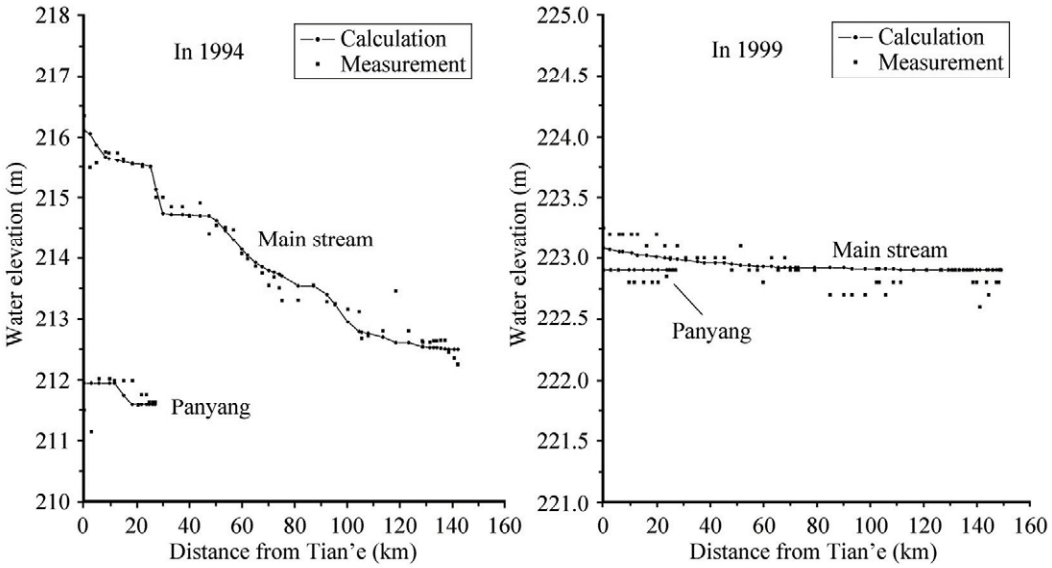

Fig. 2 Comparison of water level between calculation and measurement

Table 2 Calculated and measured volumes of deposition in the Yantan Reservoir ($10^6 m^3$)

region	1994–1997		1997–1999		1999–2001	
	Calculated	Measured	Calculated	Measured	Calculated	Measured
1–25	94.6	85.11	12.2	11.41	3.2	7.54
25–33	16.2	27.27	13.7	14.94	8.9	7.25
33–45	69.7	68.04	19.7	19.7	15.7	4.61
45–57	7.4	14.00	2.9	15.95	2.2	7.34
Sum	187.9	194.24	48.5	62.0	30.0	26.74
Accumulated	187.9	194.24	236.4	256.24	266.4	282.98

Table 2 shows that sedimentation mainly occurred in wide river reaches. The total deposition volumes in wide river reaches were very large. The deposition volume in the upper backwater region was relative low. This agrees with the actual situation, although the calculated deposition volumes in some regions are slightly different from the measured ones. Table 2 also shows that the main deposition occurred during 1994 to 1997, accounting for more than one-half of the total. The deposition volume from 1997 to 1999 decreased, and from 1999 to 2001 further decreased.

The calculated and measured changes in bed elevation along the river from 1994 to 2001 are shown in Fig. 3. One can see that the calculated and measured bed deformations agree well, with only small differences in local areas. The main differences occur in narrow sections and upper backwater regions.

Discussion

To further investigate the applicability of the model and compare the results under various scenarios, several important factors are taken into account in the sediment deposition computation. There are three calculation scenarios: (1) that in which both flocculation and density current are considered; (2) that in which flocculation is neglected, but density current is considered; and (3) that in which density current is neglected, but flocculation is considered.

The total deposition volumes for scenarios (1) and (3) are similar. The general trends for both are that sedimentation occurs quickly in the early years, accounting for almost 70% of the total, and afterwards as the river bed lifts, the deposition rate decreases. If the density current is taken into account, the fine clay is easily transported from the reservoir, considering that bed materials affect only the middle reach of the reservoir. If flocculation is not considered, the sand particles are relatively fine, and the total deposition volume is much less than measured. In other words, flocculation plays an important role in sediment deposition, while the density current has little effect.

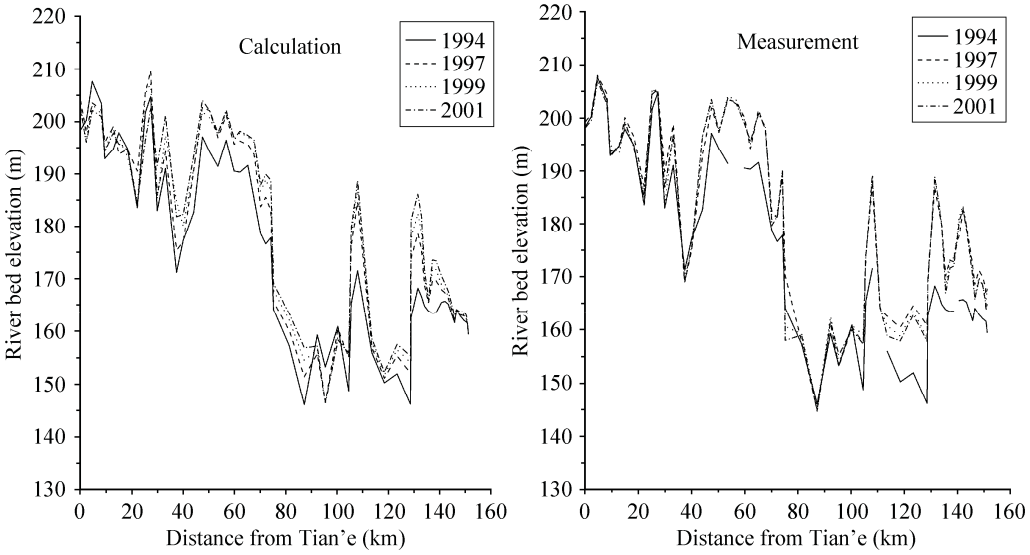

Fig. 3 Calculated and measured bed elevation changes along the river

In terms of the sediment concentration along the channel, the trends for scenarios (1) and (3) are also similar, as shown in Fig. 4. The concentration is high in the inlet section and obviously lower in the outlet section. In the middle reach and below, the concentration remains the same, therefore, the scouring and

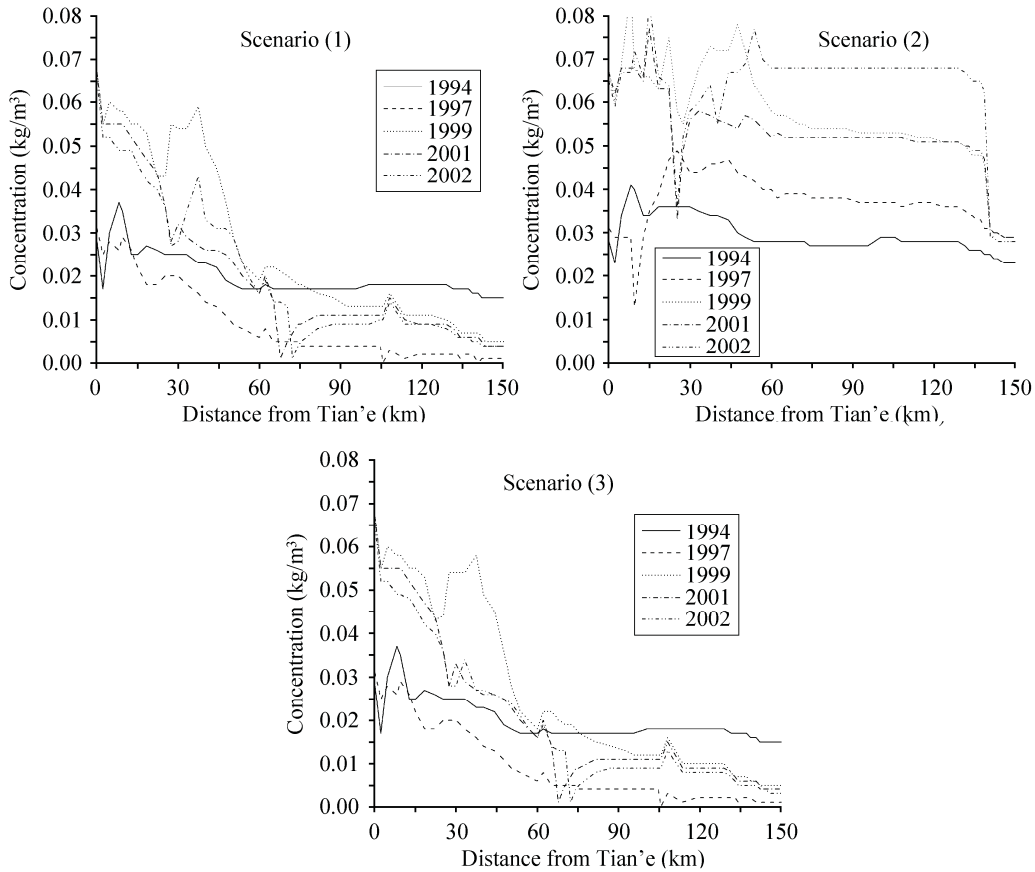

Fig. 4 Sediment concentrations along the channel in various years

filling are in equilibrium. Near the dam site, the concentration slightly decreases, therefore, some deposition occurs. There may be much deposition occurring along the channel according to the conservation of sediment. However, in scenario (2), the concentration along the channel does not vary greatly and the concentration at the outlet does not differ considerably from that at the inlet. As a result, the deposition in (2) must be less than those for the other two scenarios.

Figure 5 shows results of the averaged particle sizes of suspended load and bed material along the channel. The different results in the three scenarios are illustrated and compared. In scenario (1), the particles of sediment exiting the reservoir are mostly 0.001mm in size. The coarse particles exiting the reservoir are limited with the quantity decreasing, as the development of deposition. In the early years after reservoir operation, the average grain sizes of suspended load and bed materials differed considerably. As the suspended load enters the reservoir, its size soon becomes fine. As deposition develops, the size of suspended load approaches that of bed material. After 1999, they are still different, hence deposition continues to occur. In scenario (2), there is no flocculation; hence the grain sizes vary between 0.001mm and 0.005mm. The suspended load becomes fine after a long distance. However, the load doesn't present any measurable degree of predictable uniformity. Scenario (3) is similar to scenario (1). The main difference is that the amount of fine clay transported to the dam is less than that in scenario (1), and the average particle sizes of bed materials along the channel are not uniform. All these results reveal that after taking into account density current, the simulated depositional form and bed elevation agree well with the actual situation.

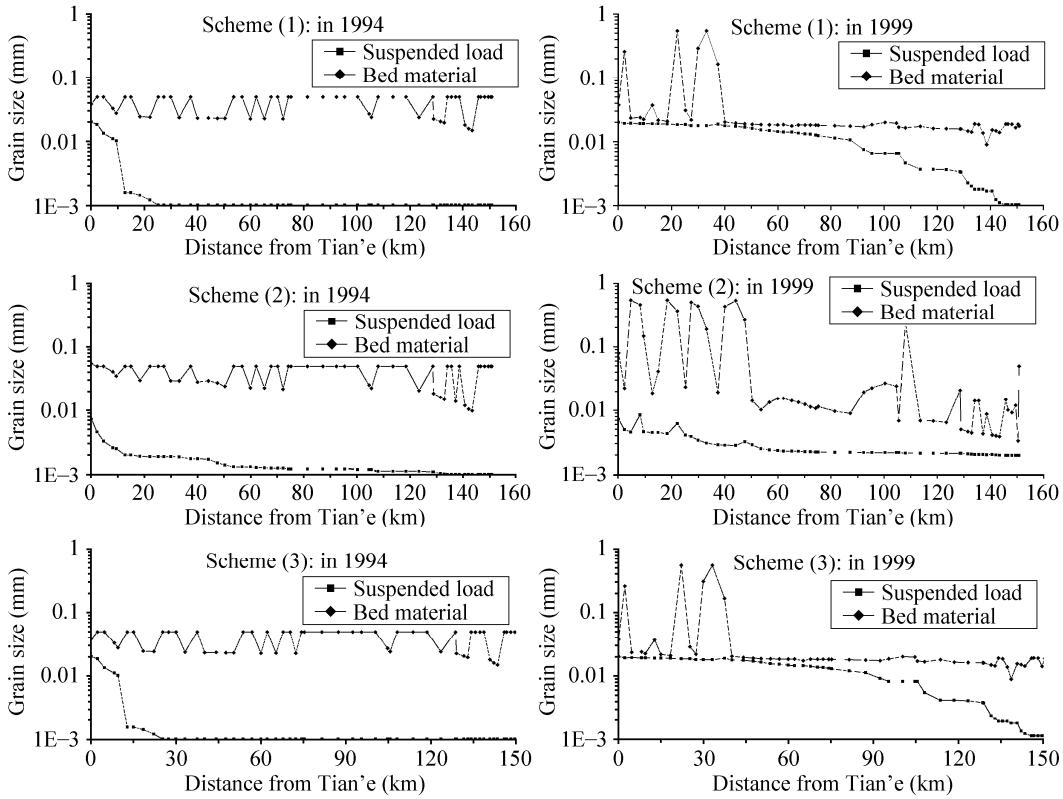

Fig. 5 Average particle sizes of suspended load and bed material along the channel

4.2 Sanmenxia reservoir calculations

Sanmenxia Reservoir is located in the middle of the Yellow River, which is well known for its high suspended-sediment concentrations. The drainage basin of this reservoir is about 688,400km^2 with average annual runoff being 46.4 billion m^3 and sediment 1.56 billion t. A 113.7 km stretch of the river reach from Tongguan Station to the Sanmenxia Dam, including 23 cross sections, is studied and simulated.

Boundary conditions

The channel topography of the Yellow River at the beginning of 1965 is used as the initial channel data. The calculation period covers from the beginning of 1965 to the end of 1966. The upstream boundary condition is flow discharge $Q(t)$ and sediment discharge $S(t)$ at Tongguan Station. The control water elevation of the Sanmenxia Dam is used as the downstream boundary condition (Chen et al., 2004).

Water elevation and sedimentation results

Both the steady and unsteady models are tested in the calculation of flow and sediment transport. For the flow model, the calculated water elevations at Tongguan and Shijiatan are chosen to compare with observed data, shown in Table 3. The agreement between the results calculated using the steady and unsteady models, and the observed data is satisfactory.

Table 3 Comparison of Tongguan and Shijiatan water elevations (m)

Time	Tongguan			Shijiatan		
	Observed	Unsteady model	Steady model	Observed	Unsteady model	Steady model
1965.11.11	327.65	326.96	327.64	307.28	307.24	307.28
1966.06.19	327.97	327.04	328.39	302.66	302.71	302.66

The total volume of deposition in the whole channel reach is chosen for sediment transport model calibration. The unsteady model (Eq. (20)) including the $\partial S/\partial t$ term and the steady model (Eq. (14)) excluding the $\partial S/\partial t$ term are applied. It can be seen from Table 4 that the unsteady model results are more accurate than the steady model results when compared with the observed data.

Table 4 Sedimentation comparison ($10^6 m^3$)

Time	From Tongguan to Shijiatan		
	Measured	Unsteady model	Steady model
65.06–65.10	–111	–118	–146
65.10–66.06	–88	–39	–21
66.06–66.10	+165	+131	+110

5 Conclusions

This paper presents a one-dimensional numerical model for unsteady flow and non-uniform sediment transport in alluvial rivers. The model calculates the unsteady flow in open channels using the Preissmann implicit method and the Thomas algorithm. Some important parameters, such as the recovery coefficient, adaptation length and sediment transport capacity, are evaluated and discussed. The recovery coefficient and sediment transport capacity are the key coefficients in hyperconcentrated flow with fine suspended sediment transport. The adaptation length should be carefully selected in a calculation of bed load transport. The model has been applied to the Hongshui River and the Yellow River, in China. The good agreement between calculations and measurements of the water surface and bed deformation demonstrates the applicability of this model.

References

Armanini A. and Di Silvio G. 1988, A one-dimensional model for the transport of a sediment mixture in non-equilibrium conditions. Journal of Hydraulic Research, IAHR, Vol. 26, No. 3, pp. 275–292.

Bell S. G. and Sutherland A. J. 1983, Non-equilibrium bed load transport by steady flows. Journal of Hydraulic Engineering, ASCE, Vol. 109, No. 3, pp. 353–367.

Cao R. X. 1979, Study on sediment transport capacity for sediment-laden flow with high silt concentration. Water Resource and Hydropower Engineering, No. 5, pp. 55–61 (in Chinese).

Chang H. H. 1982, Mathematical model for erodible channels. Journal of Hydraulic Engineering, ASCE, Vol. 108, No. 5, pp. 678–689.

Chen Q. H., Fang H. W., and Wang G. Q. 2004, 1-D numerical simulation of unsteady flow and non-uniform sediment transport at the Sanmenxia reservoir in the Yellow River. Advances in water science, Vol. 15, No. 2, pp. 160–164.

Chien N. and Wan Z. H. 1988, Sediment Transport Mechanics. Chinese Science Press (in Chinese).

Cunge J. A., Holly F. M. Jr., and Verwey A. 1980, Practical Aspects Computational River Hydraulics. Pitman Publishing Inc., Boston, MA, USA.

Einstein H. A. 1942, Formula for the transportation of bed load. Trans. ASCE, 107, pp. 561–597.
Engelund F. and Fredsoe J. 1976, A monograph on sediment transport in alluvial streams. Teknisk Verlag, Copenhagen, Denmark.
Fei X. J. 1991, A model for calculation viscosity of sediment carrying flow in the middle and lower Yellow River. Journal of Sediment Research, No. 2, pp. 1–13 (in Chinese).
Han Q. W. 1980, A study on the non-equilibrium transportation of suspended load. Proc., the First International Symposium on River Sedimentation, Beijing, China.
Meyer-Peter E. and Muller R. 1948, Formulas for bed-load transport. Report on Second Meeting of IAHR, Stockholm, Sweden, pp. 39–64.
Phillips B. C. and Sutherland A. J. 1989, Spatial lag effects in bed load sediment transport. Journal Hydraulic Research, Vol. 27, No. 1, pp. 115–133.
Qin W. K., Fu R. S., and Han Q. W. 1995, Research of adverse slope density current. Journal of Hydrodynamics ser. A, Vol. 10, No. 6, pp. 637–647 (in Chinese).
Rahuel J. L., Holly Chollet J. P. Belleudy P. J., and Yang G. 1989, Modeling of riverbed evolution for bedload sediment mixtures. Journal of Hydraulic Engineering, ASCE, Vol. 115, No. 11, pp. 1521–1542.
Thomas W. A. 1982, Chapter 18: Mathematical modeling of sediment movement. Gravel-bed Rivers, R.D.Hey et al., eds., John Wiley an Sons, Ltd., New York, USA.
van Niekerk A., Vogel K. R., Slingerland R. L., and Bridge J. S. 1992, Routing of heterogeneous sediments over movable bed: Model development. Journal of Hydraulic Engineering, ASCE, Vol. 118, No. 2, pp. 246–262.
van Rijn L. C. 1984, Sediment transport, Part I: bed load transport. Journal of Hydraulics Division, ASCE, Vol. 110, No. 10, pp. 1431–1456.
Wu W. 2004, Depth-averaged 2-D numerical modeling of unsteady flow and non-uniform sediment transport in open channels. Journal of Hydraulic Engineering, ASCE, Vol. 130, No. 10, pp. 1013–1024.
Wu W., Vieira D. A., and Wang S. S. Y. 2004, One-dimensional numerical model for non-uniform sediment transport under unsteady flows in channel networks. Journal of Hydraulic Engineering, ASCE, Vol. 130, No. 9, pp. 914–923.
Yalin M. S. 1972, Mechanics of sediment transport, Pergamon Press, p. 290.
Zhang R. J. 1961, River Dynamics. China Industry Press, Beijing (in Chinese).
Zhang R. J. and Xie J. H. 1993, Sedimentation Research in China–Systematic Selections. China Water and Power Press, Beijing.
Zhang D. R. and Liang Z. Y. 1994, Experimental research for effects on flocculation taken by non-uniform fine particle. Journal of Nanjing Hydraulic Research Institute. No. 1, 2, pp. 11–17 (in Chinese).